

Proceedings of the XXIII Conference on Applied Crystallography, Krynica Zdrój, Poland, September 20–24, 2015

# Microstructure and Magnetic Properties of the Classical Amorphous Alloys: $\text{Fe}_{61}\text{Co}_{10}\text{Y}_8\text{Me}_1\text{B}_{20}$ (where $\text{Me} = \text{W}, \text{Mo}$ )

P. PIETRUSIEWICZ\* AND M. NABIAŁEK

Institute of Physics, Faculty of Production Engineering and Materials Technology,  
Częstochowa University of Technology, al. Armii Krajowej 19, 42-200 Częstochowa, Poland

A study has been conducted into the effects of substituting small quantities of alloying elements (tungsten and molybdenum) on the structure and magnetic properties of classical amorphous alloys that are based on the formula:  $\text{Fe}_{61}\text{Co}_{10}\text{Y}_8\text{Me}_1\text{B}_{20}$ . The structure of the resulting alloy samples was examined using X-ray diffraction, Mössbauer spectroscopy, and scanning electron microscopy. Based on the results of these studies, it was found that the obtained alloys were amorphous. Images from the scanning electron microscope were typical for amorphous materials. Cross-sectional images were homogeneous and did not contain “vein- and scale-type” precipitations. Studies examining the magnetic properties of the samples were carried out using a vibrating sample magnetometer. It was found that the alloy featuring the addition of tungsten exhibited a significantly greater saturation of magnetization and a substantially lower coercivity. This resulted from the fact that the atomic radius of tungsten is much larger than that of molybdenum, resulting in increased difference between the atomic constituents of the alloy; this, in turn, improves the glass-forming ability.

DOI: [10.12693/APhysPolA.130.920](https://doi.org/10.12693/APhysPolA.130.920)

PACS/topics: 75.50.Kj, 75.50.Bb, 75.50.Lk, 75.50.-y, 61.43.Dq, 61.43.-j, 68.37.Hk, 75.70.Ak

## 1. Introduction

The amorphous materials possess excellent functional characteristics, facilitating their application in many industries [1, 2]. One particular class of the amorphous materials is that of ferromagnetic alloys, which exhibit so-called “soft magnetic properties”. Depending on their chemical composition, these alloys exhibit high values of saturation magnetization and magnetic permeability, low values of core losses and almost zero magnetostriction [3]. These functional parameter values support application of the materials in the electrotechnical industries. At present, only a few amorphous alloys are being manufactured in ribbon-form on an industrial scale; they are used mainly as materials for energy-efficient transformer cores [4]. In addition, due to their property of almost zero magnetostriction, cores made from these materials are well suited to operation at high frequencies. Research into new chemical compositions and investigation of even small changes in inherent properties are both considered priorities. In the future, such work could lead to the development of a new alloy, exhibiting excellent glass-forming ability combined with hitherto unattained soft magnetic properties.

This paper describes a study into the microstructure and magnetic properties of the alloys:  $\text{Fe}_{61}\text{Co}_{10}\text{Y}_8\text{Me}_1\text{B}_{20}$  ( $\text{Me} = \text{W}, \text{Mo}$ ). It has been found that even a minor change in the composition (1 at.%) leads to significant changes in the functional parameters of the resulting soft amorphous ferromagnet.

## 2. Experimental procedure

The samples used in the investigations were produced in the form of ribbons using high purity components ( $\approx 99.99$  at.%) combined with uni-directional cooling of the liquid alloy on a rotating copper cylinder, i.e. the melt-spinning method. The obtained ribbons were subjected to microstructure investigations using X-ray diffractometry, Mössbauer spectrometry and transmission electron microscopy. Composition analysis was performed using an EDS attachment connected to a scanning electron microscope (SEM). The magnetization changes were measured, as a function of magnetic field, using a vibrating sample magnetometer (VSM). All measurements were taken for low-energy powdered samples, which in the case of the microstructural investigations allowed information to be obtained from the whole volume of the sample, and in the case of the  $M-H$  measurements allowed the demagnetization factor, associated with the shape of the sample, to be neglected.

## 3. Results of the investigations

Figure 1 reveals the X-ray diffraction patterns for the samples of the investigated alloys in the as-quenched state. The X-ray diffraction patterns for the investigated alloys consist only of a single broad maximum, which is present at the  $2\theta$  range from  $35^\circ$  to  $55^\circ$ , and a background, which is independent of the  $2\theta$  angle [5]. This shape of diffraction pattern is characteristic for the amorphous materials.

The microstructure of the produced materials was investigated also by means of the Mössbauer spectroscopy. The transmission Mössbauer spectra (Fig. 2a,b) are wide, and consist of asymmetrical, overlapping lines, which is typical for the amorphous alloys [6, 7].

\*corresponding author; e-mail: [pietrusiewicz@wip.pcz.pl](mailto:pietrusiewicz@wip.pcz.pl)

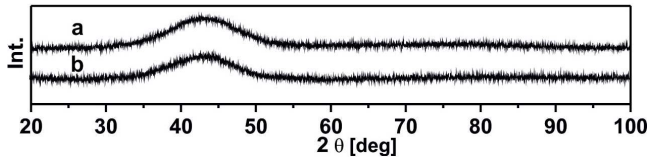


Fig. 1. X-ray diffraction patterns for the ribbon-form samples of the investigated alloys:  $\text{Fe}_{61}\text{Co}_{10}\text{Y}_8\text{W}_1\text{B}_{20}$  (a) and  $\text{Fe}_{61}\text{Co}_{10}\text{Y}_8\text{Mo}_1\text{B}_{20}$  (b).

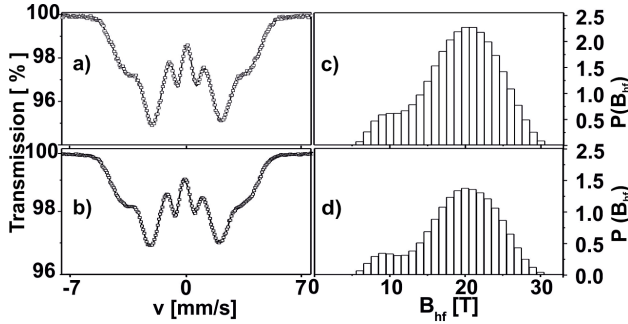


Fig. 2. The transmission Mössbauer spectra (a,b) and corresponding hyperfine field distribution (c,d) for the ribbon-shaped samples of the investigated alloys:  $\text{Fe}_{61}\text{Co}_{10}\text{Y}_8\text{W}_1\text{B}_{20}$  (a,c) and  $\text{Fe}_{61}\text{Co}_{10}\text{Y}_8\text{Mo}_1\text{B}_{20}$  (b,d).

In the corresponding hyperfine field distributions on the  $^{57}\text{Fe}$  nuclei (Fig. 2c,d) low- and high-field components can be distinguished, which indicate zones of differing iron-content in the volume of the sample [8].

The following parameters are gathered in Table I: average hyperfine field ( $B_{eff}$ ) and dispersion of the hyperfine field distribution on the  $^{57}\text{Fe}$  nuclei of the amorphous phase ( $D_{am}$ ) calculated from the Mössbauer spectra analysis.

TABLE I

The average value of the hyperfine field on the  $^{57}\text{Fe}$  nuclei ( $B_{eff}$ ) and dispersion of the hyperfine field distribution of the amorphous phase ( $D_{am}$ )

Composition	$B_{eff}$ [T]	$D_{am}$ [T]	Ref.
$\text{Fe}_{61}\text{Co}_{10}\text{Y}_8\text{W}_1\text{B}_{20}$	19.19	5.004	[9]
$\text{Fe}_{61}\text{Co}_{10}\text{Y}_8\text{Mo}_1\text{B}_{20}$	19.27	4.949	

Both the average hyperfine field and dispersion of the hyperfine field distribution on the  $^{57}\text{Fe}$  nuclei of the amorphous phase have similar values for the investigated alloys, and it is difficult to find any influence of the 1 at.% of Me on these parameters. This is due to the almost-equal covalent radius for the W and Mo components. In this case, the atomic packing densities for the alloys are similar and could be determined indirectly from  $B_{eff}$ .

The results of the chemical composition analysis of the ribbons, obtained from the EDS measurements, are presented in Fig. 3. From the calculations, it was postulated that both of the investigated alloys are homogeneous and their chemical compositions are consistent with their formulae,  $\text{Fe}_{61}\text{Co}_{10}\text{Y}_8\text{W}_1\text{B}_{20}$  and  $\text{Fe}_{61}\text{Co}_{10}\text{Y}_8\text{Mo}_1\text{B}_{20}$ .

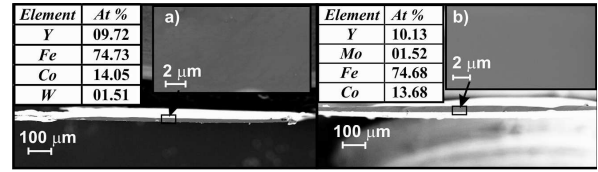


Fig. 3. The selected areas of cross-section of the ribbons (a,b) and EDS microanalysis of their chemical composition:  $\text{Fe}_{61}\text{Co}_{10}\text{Y}_8\text{W}_1\text{B}_{20}$  (a) and  $\text{Fe}_{61}\text{Co}_{10}\text{Y}_8\text{Mo}_1\text{B}_{20}$  (b).

The analysis was performed under the assumption that the data in the tables in Fig. 3 represent 80% of the composition and the remaining 20% is element B (boron). In Fig. 3a,b, cross-section images of the investigated ribbons are presented; these images were obtained using the SEM. Morphology of these cross-sections, after decohesion, is characteristic of brittle materials. In the case of the amorphous materials, this type of cross-section is observed after their thermal treatment at a temperature close to the crystallization temperature ( $T_x$ ) (mainly primary crystallization). The crystallization process in the FeCoYMeB-type alloy consists of two-stages: primary and secondary crystallization [10]. The changes in the plasticity of the amorphous alloys, especially with regard to ductility, result from the structural changes within the amorphous state. The highest ductility could be found for the alloys with “vein-based” cross-sections, then “flakes” and “smooth” cross-sections. Due to the metastable character of the amorphous alloys, especially the so-called “bulk amorphous alloys”, different atomic configurations within their volume could be found. That is why, unlike for the cross-sections for the ribbons, cross-sections of bulk amorphous alloys exhibit mixed morphology.

From the presented results of the microstructural investigations for the  $\text{Fe}_{61}\text{Co}_{10}\text{Y}_8\text{W}_1\text{B}_{20}$  and  $\text{Fe}_{61}\text{Co}_{10}\text{Y}_8\text{Mo}_1\text{B}_{20}$  amorphous alloys, it could be stated that the addition of Me (Me=W, Mo) in the volume of 1 at.% has no visible influence on the microstructure of the samples. However, a larger difference was observed in the case of the magnetic properties of the ribbons, i.e. saturation magnetization ( $\mu_0 M_S$ ) and coercivity ( $H_c$ ). The  $M-H$  measurements indicated that these parameters are strongly influenced by 1 at.% of the alloying elements [11].

Figure 4 presents static hysteresis loops, measured in magnetic fields of up to 2 T. In both cases, these loops are very narrow, and achieved the state of saturation in very low values of magnetic field, which is typical for soft magnetic materials [11]. The high values of saturation magnetization obtained for the investigated alloys were unexpected, as the samples contain 8 at.% of element Y, which is known (at just 6 at.%) to decrease the saturation magnetization ( $\mu_0 M_S$ ) [12]. It should be emphasized that the clear increase in the value of the ( $\mu_0 M_S$ ) was observed for the sample with 1 at.% of W, achieving 1.5 T; for the second sample (containing Mo), the corresponding value was lower by 0.2 T.

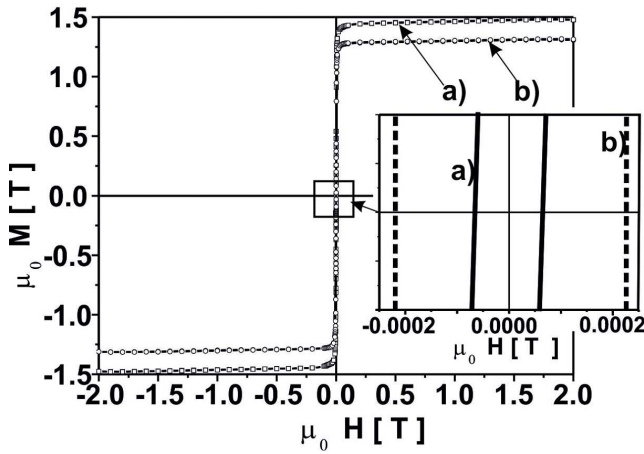


Fig. 4. Static hysteresis loops for the investigated samples:  $\text{Fe}_{61}\text{Co}_{10}\text{Y}_8\text{W}_1\text{B}_{20}$  (a) and  $\text{Fe}_{61}\text{Co}_{10}\text{Y}_8\text{Mo}_1\text{B}_{20}$  (b).

This effect was observed previously in [12], when the addition of a few at.% of element W was studied. It was also found that at some point of adding element W, the soft magnetic properties of the alloy begin to deteriorate. The addition of 1 at.% of W also has an influence on the threefold reduction in the value of coercivity, in comparison with the alloy containing Mo (Fig. 5). Data from analysis of the static hysteresis loops are gathered in Table II.

TABLE II

Data from the analysis of the static hysteresis loops.

Composition	As-quenched state		
	$\mu_0 M_S$ [T]	$H_c$ [A/m]	Ref.
$\text{Fe}_{61}\text{Co}_{10}\text{Y}_8\text{W}_1\text{B}_{20}$	1.50	61	[13]
$\text{Fe}_{61}\text{Co}_{10}\text{Y}_8\text{Mo}_1\text{B}_{20}$	1.31	186	

#### 4. Conclusions

A melt-spinning technique facilitated the production of amorphous alloy samples, in ribbon-form, with the chemical compositions:  $\text{Fe}_{61}\text{Co}_{10}\text{Y}_8\text{W}_1\text{B}_{20}$  and  $\text{Fe}_{61}\text{Co}_{10}\text{Y}_8\text{Mo}_1\text{B}_{20}$ . Amorphicity of the samples was confirmed by X-ray diffraction and Mössbauer measurements. A very interesting finding is that thin ribbons with a thickness of about 30  $\mu\text{m}$  have smooth cross-sections, which is typical for materials after an annealing process at a temperature close to the crystallization temperature [11]. This type of morphology suggests that samples of the investigated alloys are partially relaxed. Structural relaxations, occurring during the production process, led to re-configuration of the atomic positions in the volume of the ribbon, in comparison to amorphous alloys with the same thickness but different chemical composition [14]. The presence of 8 at.% of Y has an influence on the mechanical properties of the alloy, improving the microhardness of the samples but unfortunately lowering the wear resistance [15]. The amorphous ribbon

of  $\text{Fe}_{61}\text{Co}_{10}\text{Y}_8\text{W}_1\text{B}_{20}$  exhibited a higher value of saturation magnetization, and relatively low value of coercivity compared with the other sample. The small (just 1 at.%) addition of the alloying elements could be a deciding factor in determining the soft magnetic properties of the alloy, which should be remembered when designing new chemical compositions for special applications. Due to the similar atomic radii of the Mo and W additives, their influence on Fe–Fe and Co–Co atomic pair interactions is not thought to be significant; therefore, the changes in the microstructure, and magnetic and mechanical properties, cannot be explained by the changes in radii [16]. However, it is well known that the addition of element Mo results in a decrease in the Curie temperature and saturation magnetization of an alloy. This means that its presence in the alloy destabilizes the strength of the ferromagnetic exchange interactions, which was observed in this work.

#### References

- [1] M.E. McHenry, M.A. Willard, D.E. Laughlin, *Prog. Mater. Sci.* **44**, 291 (1999).
- [2] S. Lesz, R. Szewczyk, D. Szewiczek, A. Bieńkowski, *J. Mater. Process. Tech.* **157-158**, 743 (2004).
- [3] M.A. Willard, M. Daniil, in: *Handbook of Magnetic Materials*, Vol. 21, Ed. K.H.J. Buschow, North Holland, London 2013, p. 173.
- [4] S. Roth, M. Stoica, J. Degmova, U. Gaitzsch, J. Eckert, L. Schultz, *J. Magn. Magn. Mater.* **304**, 192 (2006).
- [5] Y.J. Yang, Q.J. Chen, S.S. Shan, H.W. Liu, L.M. Qiao, C.X. Liu, *J. Alloys Comp.* **480**, 329 (2009).
- [6] B.X. Gu, D.S. Xue, B.G. Shen, F.S. Li, *J. Magn. Magn. Mater.* **167**, 105 (1997).
- [7] D. Szewiczek, S. Lesz, *J. Mater. Process. Tech.* **162-163**, 254 (2005).
- [8] L.F. Kiss, J. Balogh, L. Bujdosó, D. Kaptás, T. Kemény, A. Kovács, I. Vincze, *J. Alloys Comp.* **509**, S188 (2011).
- [9] P. Pietrusiewicz, K. Błoch, M. Nabiałek, S. Walters, *Acta Phys. Pol. A* **127**, 397 (2015).
- [10] J. Han, C. Wang, Sh. Kou, X. Liu, *Trans. Non-ferr. Met. Soc. China* **23**, 148 (2013).
- [11] M.G. Nabiałek, M. Szota, M.J. Dospial, *J. Alloys Comp.* **526**, 68 (2012).
- [12] P. Pietrusiewicz, M. Nabiałek, M. Szota, K. Perduta, *Arch. Metall. Mater.* **57**, 265 (2012).
- [13] M. Nabiałek, P. Pietrusiewicz, K. Błoch, *J. Alloys Comp.* **628**, 424 (2015).
- [14] Yong Ik Jang, Jongryoul Kim, Dong Hyuk Shin, *Mater. Sci. Eng. B Solid* **78**, 113 (2000).
- [15] I. Betancourt, S. Baez, *J. Non-Cryst. Solids* **355**, 1202 (2009).
- [16] H. Kronmüller, *J. Appl. Phys.* **52**, 1859 (1981).